CORA Cork Open Research Archive
Cartlann Taighde Oscailte Chorcaí

Title	Establishing experimental parameters for biphasic transfer in vitro lipolysis model
Authors	Kirschbaum, Hannah S.;Jede, Christian;Koehl, Laura J.;Kuentz, Martin;Holm, René;Griffin, Brendan T.;Blechar, Johannes A.;ÓDwyer, Patrick J.
Publication date	2026-07-10
Original Citation	Kirschbaum, H S, Jede, C, Koehl, L J, Kuentz, M, Holm, R, Griffin, B T, Blechar, J A & ÓDwyer, P J 2026, 'Establishing experimental parameters for biphasic transfer in vitro lipolysis model', International Journal of Pharmaceutics, vol. 700, 127051, pp. 1-12. https://doi.org/10.1016/j.ijpharm.2026.127051
Type of publication	Article (peer-reviewed)
Link to publisher's version	https://www.scopus.com/pages/publications/105041786764 - 10.1016/j.ijpharm.2026.127051
Rights	© 2026, authors. Published by Elsevier B.V. This is an open access article under the CC BY license (http://creativecommons.org/licenses/by/4.0/) - https://creativecommons.org/licenses/by/4.0/
Download date	2026-11-17 04:25:27
Item downloaded from	https://hdl.handle.net/10468/19437

UCC
University College Cork, Ireland
Coláiste na hOllscoile Corcaigh

International Journal of Pharmaceutics 700 (2026) 127051

Contents lists available at ScienceDirect

International Journal of Pharmaceutics

journal homepage: www.elsevier.com/locate/ijpharm

Establishing experimental parameters for biphasic transfer in vitro lipolysis model

Hannah S. Kirschbaum [a,b], Christian Jede [c], Laura J. Koehl [a], Martin Kuentz [d], René Holm [e], Brendan T. Griffin [b], Johannes A. Blechar [a], Patrick J. ÓDwyer [b,*]

[a] Global Analytical Development, Global CMC Development, Merck Healthcare KGaA, Frankfurter Strasse 250, 64293 Darmstadt, Germany
[b] School of Pharmacy, University College Cork, Cork, Ireland
[c] Clinical Pharmacology, Quantitative Pharmacology, Merck Healthcare KGaA, Frankfurter Strasse 250, 64293 Darmstadt, Germany
[d] Institute for Pharma Technology and Biotechnology, University of Applied Sciences and Arts Northwestern Switzerland, Hofackerstr. 30, Muttenz 4132, Switzerland
[e] Department of Physics, Chemistry and Pharmacy, University of Southern Denmark, Campusvej 55, 5230 Odense, Denmark

ARTICLE INFO

Keywords:
Gastrointestinal transfer
In vitro digestion
Lipid-based formulations
Biphasic lipolysis
Supersaturation
Absorption

ABSTRACT

Lipid-based–formulations (LBFs) are widely used to improve oral bioavailability of poorly water–soluble drugs. Despite their widespread use in predicting formulation performance, standard *in vitro* lipolysis assays often lack an absorptive sink and fail to capture the transition from gastric to intestinal environments, thereby reducing their predictive relevance for *in vivo* outcomes. The aim of this study was to develop a biphasic *in vitro* lipolysis model incorporating an absorptive sink. This might offer the potential to increase the predictive power of *in vitro* digestion models in the future. In this model, the absorptive sink was provided by a decanol layer, and to simulate gastrointestinal transit, two dynamic pH–transition approaches were employed: a biphasic GI–transfer model and a biphasic pH–shift model. Using nilotinib–loaded LBFs, the study established conditions for this biphasic system and examined how media composition and lipase source influence drug concentrations during formulation dispersion, digestion, and partitioning into the organic sink. The results showed that digestion experiments conducted with either porcine pancreatin or Palatase® 20000 L increased the concentration of nilotinib in the aqueous digestion medium, which correspondingly reduced partitioning of the drug into the decanol layer. For the readily dispersible Type III LBF in the biphasic GI–transfer setup, nilotinib permeation into the decanol layer decreased compared with a lipid–free control, likely due to improved drug solubilization in the aqueous digestion phase. In contrast, the poorly dispersible Type I LBF was better suited to the biphasic pH–shift setup, but it showed higher drug levels in the decanol layer, reflecting rapid partitioning of lipids—and associated crystalline drug—into the organic phase. Overall, this study establishes suitable conditions for evaluating the lipolysis of LBFs during a dynamic pH transition in the presence of an absorptive sink. This advanced approach provides additional insight to explore digestion–mediated and/or pH–mediated supersaturation during digestion of LBFs.

1. Introduction

The rise of poorly water-soluble drug candidates, classified as Biopharmaceutical Classification System (BCS) class II and IV compounds, poses significant challenges for achieving adequate oral bioavailability in pharmaceutical formulations (Ting et al., 2018; Hashmi et al., 2025). Many enabling formulation strategies, such as particle size reduction, generation of solid dispersions, or salt formation, primarily address the poor water solubility (Stegemann et al., 2023; Kuentz et al., 2021); while approaches that also enhance intestinal permeability remain comparatively limited (Feeney et al., 2016). Another strategy to increase the apparent gastrointestinal solubility is the use of lipid-based formulations (LBFs) (Bourderi-Cambon et al., 2025; Bennett-Lenane et al., 2020; Ueda et al., 2026). In addition, LBFs can favourably influence drug permeation, by potentially modulating membrane fluidity, transiently opening tight junctions or reducing P–glycoprotein–mediated efflux, thereby enhancing drug permeation across the intestinal mucosa (Berthelsen et al., 2019; Weinheimer et al., 2017; Lindmark et al., 1998). A key

* Corresponding author at: School of Pharmacy, University College Cork, Cork, Ireland.
E-mail address: Patrick.odwyer@ucc.ie (P.J. ÓDwyer).

https://doi.org/10.1016/j.ijpharm.2026.127051
Received 25 March 2026; Received in revised form 23 May 2026; Accepted 2 June 2026
Available online 8 June 2026
0378-5173/© 2026 The Author(s). Published by Elsevier B.V. This is an open access article under the CC BY license (http://creativecommons.org/licenses/by/4.0/).

advantage of LBFs is their ability to generate drug supersaturation on digestion and dispersion within the intestinal fluids (Vinarov et al., 2021). While supersaturation can enhance absorption, it may also promote precipitation, ultimately limiting absorption. To support formulation selection, *in vitro* tools play an important role in gaining mechanistic insights into drug release, precipitation, re-dissolution, and absorption behaviour (Berthelsen et al., 2019; O'Dwyer et al., 2019).

The complexity of these *in vitro* lipolysis models varies depending on the development stage and the specific scientific questions being addressed, with different setups capturing distinct aspects of lipid digestion. In early–stage development, the well–established pH–stat lipolysis model is frequently used (Sek et al., 2002; Zangenberg et al., 2001; Williams et al., 2012). However, although well established, the pH-stat and other existing *in vitro* setups often overestimate the extent of drug precipitation and can consequently underpredict the *in vivo* exposure of LBFs (Berthelsen et al., 2019; Griffin et al., 2014). Kirschbaum et al. (2025) demonstrated that pH-stat lipolysis can produce extensive precipitation *in vitro*, up to 70% of the drug, while *in vivo* exposure in rats was substantially higher (>50%). Thus, extensive precipitation observed in a one-pot pH-stat system does not necessarily predict reduced *in vivo* exposure. The possible causes of overprediction of drug precipitation in many *in vitro* models, particularly for weak bases, are the omission of a gastric step and/or a missing absorption phase.

Accordingly, several models now include a gastric dissolution and/or digestion prior to digestion in the simulated small intestinal compartment (Fernandez et al., 2009; Klitgaard et al., 2020; Siqueira Jorgensen et al., 2018; Christophersen et al., 2014; Fiolka et al., 2020; Siqueira Jorgensen et al., 2019). Klitgaard et al. (2020) showed that adding a gastric dispersion step improved the prediction of pharmacokinetic data compared to a one-step intestinal digestion model. Sassene et al. (2016) reported extensive precipitation of danazol and fenofibrate in rat gastric contents after administration in lipid–based formulations, demonstrating that processes occurring in the stomach can strongly influence downstream solubility and precipitation, making a gastric step relevant for *in vitro* models. Another example is the developed rat gastrointestinal lipolysis model by Siqueira Jorgensen et al. (2018), which was able to show that the simulation of the gastric stage enhanced prediction.

The second key limitation of existing lipolysis models is the absence of a simulated absorptive compartment, causing many *in vitro* transfer assays to overpredict the extent of drug precipitation in the luminal phase (Griffin et al., 2014; Stillhart and Kuentz, 2016). Several *in vitro* concepts have been developed to mimic drug absorption in the small intestine, ranging from small-scale permeation devices such as the PermeaLoop™ system (Sironi et al., 2018) or the use of a Permeapad® barrier (Sirvi et al., 2024; Klitgaard et al., 2021) to multi-compartment simulators such as the TNO Gastro-Intestinal Model (TIM) (Lopez Marmol et al., 2026). Another widely used approach is to incorporate an organic layer on top of the aqueous donor medium to generate sink conditions in the donor medium. Biphasic dissolution setups have proven valuable for characterizing the dissolution-partitioning behaviour of solid dosage formulations (Brenner et al., 2024; Mudie et al., 2012; Deng et al., 2017). For example, Denninger et al. (2020) applied a biphasic one–vessel assay to study the absorption of a ritonavir amorphous solid dispersion and demonstrated that dissolution–partitioning profiles were highly dependent on fasted–state media composition, particularly bile salt concentration. Furthermore, Jede et al. (2023) demonstrated that the degree of drug precipitation of a poorly and pH-dependent soluble BCS class II weakly basic drug could be much more accurately predicted using a dissolution-transfer-partitioning system (DTPS). Using this approach, the authors were able to reliably estimate the drug's dose proportionality in agreement with Phase 1 clinical data.

However, translating biphasic approaches from solid dosage forms to LBFs introduces additional biophysical and experimental challenges in drug delivery. There are formulation specific aspects that need to be evaluated, since the components like lipids and surfactants have the potential to interact with the organic phase (Stillhart and Kuentz, 2016). O'Dwyer et al. (2020) were the first to describe the use a biphasic lipolysis system to investigate LBFs containing nilotinib, fenofibrate and danazol. The authors demonstrated that a biphasic lipolysis method containing digestive enzymes in simulated intestinal fluid provided valuable predictions of *in vivo* performance (O'Dwyer et al., 2020). Nonetheless, this one–compartment method was not suitable for assessing physiological transition from gastric to intestinal conditions; as a result, it may not accurately estimate the solubility and supersaturation behaviour of drugs that are sensitive to pH transitions from the gastric to intestinal environment (Mathias et al., 2013).

The aim of the present study was to evaluate the drug behaviour in a biphasic lipolysis model that integrated a gastrointestinal transfer mechanism with an organic absorptive sink compartment, thereby addressing the two limitations of conventional *in vitro* lipolysis assays. Two set ups were explored: a biphasic GI–transfer lipolysis system incorporating first–order simulated gastric emptying into intestinal medium, and a biphasic pH–shift model in which conditions transition rapidly from gastric to intestinal. Nilotinib was selected as the model drug due to its physicochemical characteristics: a weakly basic, poorly water–soluble compound with pH–dependent solubility (pKa 3.9 and 5.1–5.6; solubility of 118 μg/mL in SGF at pH 2.0 and 0.6 μg/mL in FaSSIF pH 6.5[18]), low permeability, and high lipophilicity (logP 5.0) (Koehl et al., 2019). The present study evaluated how i) media composition, ii) lipase source, and iii) LBF type affected nilotinib solubilization, supersaturation, precipitation and partitioning into an absorptive layer. Notably, this study also incorporated the analysis of drug and lipid concentrations in the aqueous and organic phase during the testing of poorly dispersible Lipid Formulation Classification System (LFCS) type I LBF suspensions and a supersaturated LBF in the biphasic pH-shift lipolysis model. Consequently, the present work provides new insights into the use of a biphasic GI transfer or pH-shift lipolysis assay using a model drug of BCS class VI in different LBFs.

2. Materials and methods

2.1. Chemicals

Nilotinib was purchased from abcr GmbH (Karlsruhe, Germany). The pancreatic extract (8 x USP), Tween® 85 (Polyoxyethylene Sorbitan Trioleate), Cremophor® RH40 (containing glyceryl polyethylene glycol oxystearate and fatty acid glyceryl polyglyceryl esters), sodium chloride, sodium hydroxide, hydrochloric acid 37%, sodium dihydrogen phosphate, 1-decanol and tris(hydroxymethyl)aminomethane were obtained from Merck KGaA (Darmstadt, Germany). Tricaprin was purchased from Tokyo chemical industry Co (Tokyo, Japan). Peceol® (Mono-, di- and triglycerides of oleic ($C_{18:1}$) acid, monoester fraction being predominant) was kindly donated from Gattefossè (Saint-Priest, France). The lipases Palatase® 20000 L and Novozym® 435 were purchased from Strem Chemicals Ltd. (Suffolk, UK). 3F powder for the preparation of fasted state simulated intestinal fluid (FaSSIF) was obtained from biorelevant (London, UK). All other chemicals and solvents were of analytical grade and used as received. Water used for all experiments was obtained from a MilliQ water system.

2.2. Methods

2.2.1. Preparation of media

Simulated Gastric Fluid (SGF) was adjusted to pH 2.0 or 4.0 with 1 M HCl to minimize pH reduction during the intestinal phase of the experiment (Jede et al., 2023). SGF_Ca^{2+} included an additional 1.4 mM $CaCl_2$. For the simulated intestinal medium, the biorelevant medium, FaSSIF, was prepared using a double-concentrated phosphate buffer at pH 6.5, ensuring a constant and physiologically relevant pH during GI transfer/pH–shift experiments (Jede et al., 2019). The phosphate buffer comprised 77.5 mM NaCl and 56.8 mM NaH_2PO_4. Additionally, a 20 mM Tris buffer_Ca^{2+} was prepared, incorporating 1.4 mM $CaCl_2$ and

150 mM NaCl. FaSSIF was prepared by adding 2.24 g of 3F powder to 1000 mL of either the double-concentrated phosphate or the Tris buffer (only utilized in Section 3.1.2). The preparation was conducted in accordance with the guidelines provided by biorelevant.com.

2.2.2. Solubility tests

The solubility of nilotinib in SGF (pH 2.0) and FaSSIF (pH 6.5) has been reported previously (Kirschbaum et al., 2025). The solubility of nilotinib in decanol was evaluated using the shake flask method at 37 ± 0.5 °C. An excess amount of drug substance was added to 30 mL of preheated decanol in a 50 mL flask. The flasks were placed in a water bath and shaken at 37 ± 0.5 °C. After 24 h, samples were withdrawn and centrifuged at 14,000 rpm and 37 °C for 15 min using a benchtop centrifuge (Centrifuge 5430 R with rotor FA-45-30-11, Eppendorf AG, Hamburg, Germany). The supernatant was collected and centrifuged again under identical conditions. Subsequently, the supernatant was diluted with methanol and analysed by HPLC as described in Section 2.2.5.

2.2.3. Lipase activity assay

Lipase activity was determined in accordance with the INFOGEST inter-laboratory recommendations for assaying pancreatic lipase activity (Grundy et al., 2021). The porcine pancreatic extract was freshly prepared by adding 10 mL of 5 °C blank digestion buffer (phosphate buffer without phospholipids and bile salts) to 2 g of porcine pancreatic enzymes (8 × USP) in a 50 mL falcon tube, which was then thoroughly vortexed. The mixture was centrifuged for 15 min at 5 °C and at 4500 rpm (centrifuge 5430 R with rotor FA-45–30-11, Eppendorf AG, Hamburg, Germany). The supernatant was then collected and stored on ice for subsequent use. Lipase activity was assessed immediately after preparation, following the protocol of Grundy et al. (2021), which served as a reference lipase activity. To evaluate the potential impact of the decanol layer on lipase activity, a concentration of 1000 TBU/mL of pancreatic enzymes was added to 250 mL of FaSSIF in a USP vessel, which was layered with 400 mL of decanol. The mixture was stirred at 75 rpm for 2 h at 37 ± 0.5 °C. Subsequently, samples were collected, and the lipase activity was evaluated.

2.2.4. Preparation of the LBFs

The LBFs were prepared as described previously by Kirschbaum et al. (2025) and Koehl et al. (2019); the composition of each formulation is shown in Table 1. In summary, nilotinib suspensions (10 mg/mL) were prepared by weighing and mixing the drug with the lipid excipient and stirring at 37 °C overnight. To prepare the type I supersaturated LBF (sLBF), nilotinib was added into Peceol® and heated up to 130 °C in three heating cycles to obtain a clear solution (Kirschbaum et al., 2025).

2.2.5. Biphasic GI transfer lipolysis model

For setting up the biphasic GI transfer lipolysis model, the volumetric parameters and buffer compositions were based on the dissolution-transfer-partitioning system developed by Jede et al. (2023). A schematic representation of the adapted setup is illustrated in Fig. 1A and B. 250 mL SGF was filled into a mini vessel (300 mL) and 250 mL of FaSSIF was filled into a standard (1000 mL) dissolution vessel, using an Agilent 708-DS dissolution apparatus (Agilent Technologies, Santa Clara, CA, USA). Decanol (400 mL) was added on top of the FaSSIF. A programmable peristaltic pump (ISMATEC MCP Process, IDEX Health & Science, Wertheim, Germany) connecting the mini vessel to the standard vessel allowed a physiologically relevant first-order simulated gastric emptying with a half-life of 5 min (transfer duration was 25 min). The rotation speed was set to 75 rpm and the temperature in the vessels were kept at 37 ± 0.5 °C. To allow constant stirring of the organic and the aqueous phase a 3D printed dynamic biphasic dissolution paddle device was used, developed by Jede et al. (2023). With a ratio of 1:200 for LBF: digestion medium (Bennett-Lenane et al., 2021) 2.5 g of LBF was subsequently added into SGF, using a syringe (Kirschbaum et al., 2025). A 4 mL sample was taken after 2.5 min, which was subsequently ultracentrifuged at 37 °C and 100,000 × g for 15 min (Optima™ MAX-XP, Beckman Coulter). After 5 min of dispersion, the peristaltic pump program was started, and the digestion enzyme were added into FaSSIF. The different digestion enzymes used are listed in Table 2. Titration throughout the *in vitro* lipolysis was performed using a Titrando® 907, a pH electrode (Metrohm AG, Herisau, Switzerland), and two 800 Dosino® dosing units. The system was operated by the Tiamo® 3.0 software. With the addition of the digestion enzymes the titration was started, and the experiment was monitored for 180 min. After 180 min the pH of the buffer was increased to pH 9.0 to allow for determination of all released non-ionized free fatty acids (FFA). A reference *in vitro* lipolysis experiment was carried out to analyse FFAs released by digestion of FaSSIF. The tubes and the gastric compartment were rinsed with 100 mL of SGF pH 2.0 and nilotinib concentration was determined. Samples of 1 mL of the decanol phase and samples of 4 mL of the aqueous phase were taken at 2.5, 5, 10, 15, 30, 45, 60, 90, 120, and 180 min during the digestion experiment, and lipases were inhibited by the addition of 1 M 4-Bromophenylboronic acid in methanol (5 µL per mL sample). 3.335 mL of the 4 mL was filled in a centrifugation tube and ultracentrifuged under the same conditions as the dispersion samples. The remaining sample (aqueous phase total) was used to analyse the total nilotinib concentration in the acceptor vessel and diluted 1:10 in acetonitrile and methanol (35:30, v/v). Preparation of the samples after ultracentrifugation and their subsequent dilutions were carried out according to Kirschbaum et al. (2025). The samples from the decanol phase were diluted 1:10 with pure methanol. All experiments were performed in triplicates. As described by Kirschbaum et al. (2025) the concentration of nilotinib was analysed using reverse phase HPLC.

Table 1
Overview of the composition of the nilotinib solution LBFs (drug amount of 10 mg/mL of LBF) tested in this study.

Formulation code	SGF [% in v/v]	Excipients [% in w/w]			
		Peceol®	Tricaprin	Cremophor® RH40	Tween® 85
SGF solution	100	–	–	–	–
Type III	–	–	40	20	40
Type I	–	–	100	–	–
Type I sLBF	–	–	100	–	–

2.2.6. Biphasic pH-shift lipolysis model

The biphasic pH-shift lipolysis model is designed as a one-compartmental model, in which the pH-shift is realized by the addition of the second stage dissolution medium to the same vessel instead of using two individual vessels connected by a peristaltic pump. The model was developed as an alternative to the biphasic GI transfer lipolysis model to enable testing of poorly dispersible LBFs, such as the LFCS type I LBFs, which were observed not to disperse sufficiently in SGF, i.e. floating on top of SGF and consequently not being able to be reliably transferred through tubing using standard USP transfer procedure described in Section 2.2.5 (pictures in Fig. S1, Supplementary Materials). The method combined a controlled gastric dispersion period in SGF, intestinal medium was added to generate a gastric to intestinal pH shift. The experimental conditions were established in accordance with the *in vitro* pH-shift lipolysis method outlined in Kirschbaum et al. (2025), incorporating an additional step by the introduction of a decanol layer following the addition of FaSSIF. A schematic representation of the adapted setup is illustrated in Fig. 1C and D. The protocol was similar as described in 2.2.5 with a few adaptations. The standard dissolution USP II vessel (1000 mL) was filled with 250 mL of SGF pH 2.0 (described in Section 2.2.1), and stirring was initiated at 250 rpm at 37 °C. Then, 2.5 g of LBF was added to the SGF. After 15 min of dispersion, a 4 mL sample was taken from the middle of the vessel. After 29 min, 247 mL of FaSSIF, prepared using double-

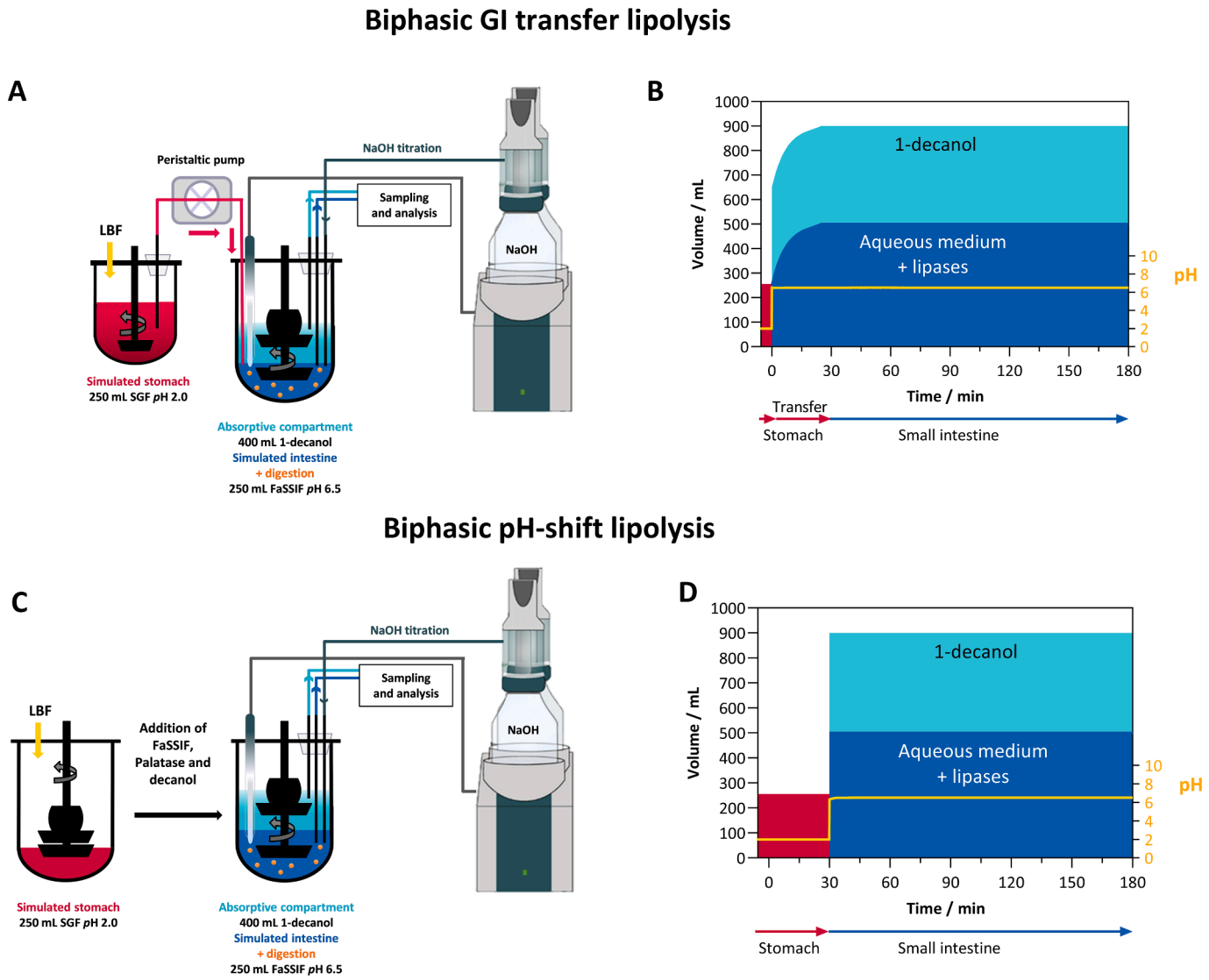


Fig. 1. Schematic representation of experimental setups A + B: The biphasic gastrointestinal transfer lipolysis setup. A is a schematic representation, including a peristaltic pump to transfer simulated stomach medium into simulated intestinal medium. B: Dissolution procedure: starting with 5 min dispersion in SGF, then the transfer into 250 mL of FaSSIF with 400 mL of decanol. C + D: The biphasic pH-shift lipolysis setup. C: The biphasic pH-shift lipolysis setup. D: Dissolution procedure: starting with 30 min dispersion in SGF, then the addition of 250 mL of FaSSIF and 400 mL of decanol. Dissolution procedures are adapted from Brenner et al. (2024).

Table 2
Used lipases during lipolysis experiments. TBU/mL expresses 1 μmol of butyric acid released per minute and PLU/mL reflects the amount of enzyme that generates 1 μmol of propyl laurate per minute.

Lipase	Form of lipase	Selectivity	Concentration used (activity/ volume of digestion medium)
Porcine pancreatin	Liquid	Sn-1,3	1000 TBU/mL[a] (Williams et al., 2012)
Novozym® 435	Immobilized	non	125 PLU/mL (Ejskjaer et al., 2024; Keemink and Bergstrom, 2018)
Palatase® 20000 L	Liquid	Sn-1,3	125 PLU/mL (Ejskjaer et al., 2024)

[a] Activity was determined with tributyrin assay described by Grundy *et al.* (Grundy et al., 2021).

concentrated phosphate buffer, was added to the dispersion. Subsequently, 3.125 mL of Palatase® 20000 L as a lipase source (125 LU/mL of digest (Ejskjaer et al., 2024)) was added, and the mixture was stirred at 250 rpm for an additional minute. The type I suspension was tested with two procedural variants: first, with a dispersion time of 5 min versus 30 min in SGF of pH 2.0, and second, with 30 min dispersion in SGF at pH 4.0. The stirring speed was then reduced to 75 rpm, and titration was initiated. The rest of the protocol remained the same, and sample collection and analysis during digestion were the same. The concentrations of the lipidic formulation components in both phases were monitored using liquid chromatography coupled with evaporative light scattering detection (ELSD). A reversed-phase HPLC-ELSD method based on a protocol from Mousli et al. (2022) was used to detect the lipids of the LBFs in the aqueous and decanol samples. HPLC utilizing a 1260 Infinity series HPLC system (Agilent Technologies, Santa Clara, CA, USA) series comprising a quaternary pump, an Agilent autosampler, a thermostat, a thermostated column compartment, and an Agilent Diode Array Detector VL and ELSD. The analytical conditions are listed in Supplementary Materials in Tables S1 and S2. For Peceol LOD and LOQ were determined based on signal to noise ratios (S/N ratios) of 9 ng/mL and 25 ng/mL, respectively, in accordance with the ICH Q2 guideline.

2.2.7. *Molecular modelling and statistics analysis*

Molecular modeling pro flavor plus, V.9.1.2 (Norgwyn Montgomery

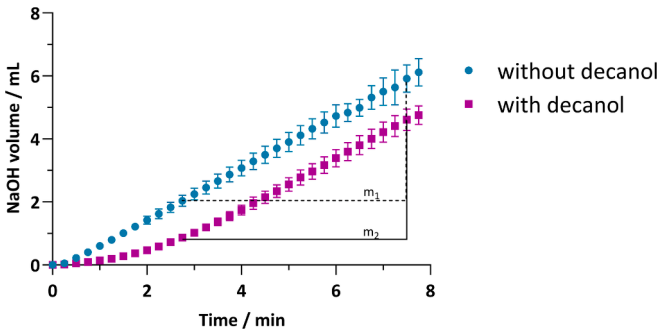


Fig. 2. NaOH delivery (mL) as a function of time (min) to determine lipase activity with slope m_2 in FaSSIF in the presence (■) or m_1 in the absence (●) of decanol layer (mean ± SD, n = 3).

Software Inc., North Wales, USA) software package was used to estimate the Hansen`s 3-Ds solubility parameter for glyceryl oleate and for decanol.

To determine the activity (μmol/min) of porcine pancreatin (see Table 2), the slope of the NaOH titration curve was determined using the time interval between $t_1 = 2.5$ to $t_2 = 7.5$ min. As described by Grundy et al. (2021), the time interval selected should cover a time period of at least 5 min, beginning after the lag time which can depend on the equipment used or on enzyme activity. Eq. (1) was used, where V_{NaOH} denotes the volume of NaOH delivered (μL), between times t_1 and t_2. N is the normality (titer) of the NaOH solution (0.1 N).

$$lipaseacitvity[\mu mol/min] = (\Delta V_{NaOH}/(t_2 - t_1))^{*}N \quad (1)$$

The specific activity of pancreatin (TBU/mg) was calculated with Eq. (2), where *C* is the concentration (mg/mL) of powder in the enzyme solution and *v* is the volume of enzyme solution that was added (μL).

$$specificactivityofpancreatin[TBU/mg] = (lipaseactivity^{*}1000)/(C^{*}v) \quad (2)$$

To determine the percentage of LBF that underwent digestion, the theoretical amount of FFAs per g of LBF was calculated using Eq. (3). The saponification value (SV), expressed in mg KOH per g of each excipient in the LBF, was obtained from the certificate of analysis. The molecular weight of KOH used in the calculation was 56.1056 g/mol.

$$Theoretical\,FFA\,[mmol] = \mathrm{SV}\,[\mathrm{mg}]/56.1056\,[\mathrm{g/mol}] \quad (3)$$

The transferred volume, the cumulative transfer and the percentage of dose present in each phase were calculated according to Jede et al. (2023). V_0 representing the initial gastric volume (t = 0) and V_n is representing the remaining gastric volume at each sample time point, (see Eqs. (4), (5) and (6)). Volume changes due to transfer, titration, and sample withdrawal were accounted for at every time point to ensure accurate concentration and mass balance calculations.

$$\text{transferred volume}\,[\mathrm{mL}] = V_0 - \left(\sum V_n\right) \quad (4)$$

$$\text{Cummulative transfer}\,[\mathrm{mg}] = \text{concentration donor}\left[\frac{\mathrm{mg}}{\mathrm{mL}}\right] {}^{*}\text{transferred volume}\,[\mathrm{mL}] \quad (5)$$

$$\%\,\text{of dose in phase X} = \text{determined mass}\,[\mathrm{mg}]/\text{cumulative transfer}\,[\mathrm{mg}]^{*}100 \quad (6)$$

Statistical analysis of the results was performed using GraphPad Prism® 10 (GraphPad Software, USA). Normality of residuals was assessed by the Shapiro–Wilk test and homogeneity of variance by Levene's test. For comparisons at individual time points involving two categorical factors (lipase source and timepoints), a two-way ANOVA was chosen. In all cases multiple comparisons were performed using Tukey's post–hoc test (α = 0.05).

3. Results and discussion

3.1. Establishing experimental conditions

3.1.1. Influence of decanol phase on lipase activity

Prior to lipolysis testing, the effect of a decanol absorptive sink on lipase activity in FaSSIF was evaluated (Section 2.2.3). The activity of freshly prepared pancreatic extract exhibited an activity of 2.47 ± 0.16 TBU/mg (see Fig. 2). After 2 h of stirring in the biphasic system containing a decanol layer, measured activity was 2.44 ± 0.19 TBU/mg, corresponding to 98.8% of initial activity. These results indicate that lipases derived from porcine pancreatin maintain their activity in the aqueous phase for at least 2 h in the presence of a decanol overlay. A consistently longer lag phase of the digestion during lipase activity determination was observed relative to that of the control (i.e. without decanol layer). One possible explanation is that small quantities of decanol may become emulsified into the aqueous phase, altering interfacial properties or droplet formation upon substrate addition. Such changes may delay effective enzyme–substrate interactions and thereby delay the onset of lipolysis because the reaction rate is governed by the composition of the interfacial microenvironment (Reis et al., 2009).

3.1.2. Influence of calcium on transition of nilotinib into the decanol layer

The potential for liberated free fatty acids (FFAs) generated during digestion to impede drug partitioning into decanol, possibly through accumulation at the aqueous–decanol interface,was evaluated. To investigate this, the influence of calcium ions in the digestion medium on drug transfer into decanol was examined, as calcium promotes precipitation of ionized FFAs (Devraj et al., 2013). The type III LBF was tested in the GI transfer lipolysis setup (see Section 2.2.5), under two conditions: calcium–containing media (SGF_Ca^{2+} and FaSSIF prepared with Tris buffer_Ca^{2+}) versus calcium–free media (SGF and FaSSIF prepared with phosphate buffer), with porcine pancreatin used as lipase source. During the first 90 min, both conditions produced essentially identical partitioning kinetics into decanol (see Fig. 3). At 180 min, decanol fractions were at 10.9 ± 1.3% with no calcium and 12.9 ± 0.6% of the dose when calcium was present (see Fig. 3). Fig. 4 shows that the presence of calcium ions in the medium increased both the magnitude and duration of nilotinib supersaturation in the aqueous phase dissolved. The precipitation of ionized FFAs as calcium soaps did not significantly affect nilotinib partitioning into decanol, indicating that any potential FFA accumulation at the aqueous–decanol interface did not hinder the drug transfer into the organic phase. Similar to findings from Ejskjaer et al. (2024), who reported preserved lipase activity under calcium-free conditions, these results justified performing subsequent experiments in calcium-free media.

3.1.3. Influence of an absorptive sink on nilotinib solubility in aqueous digest phase

The influence of a decanol overlay on the aqueous digest phase was

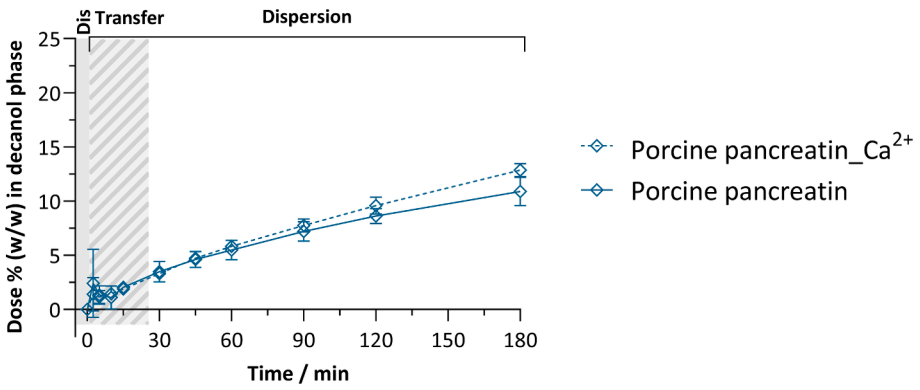


Fig. 3. Drug release time profile in decanol layer for nilotinib in type III LBF with porcine pancreatin (◊), straight line is calcium–free media, and dotted line is calcium–containing media. Means ± SD, n = 3.

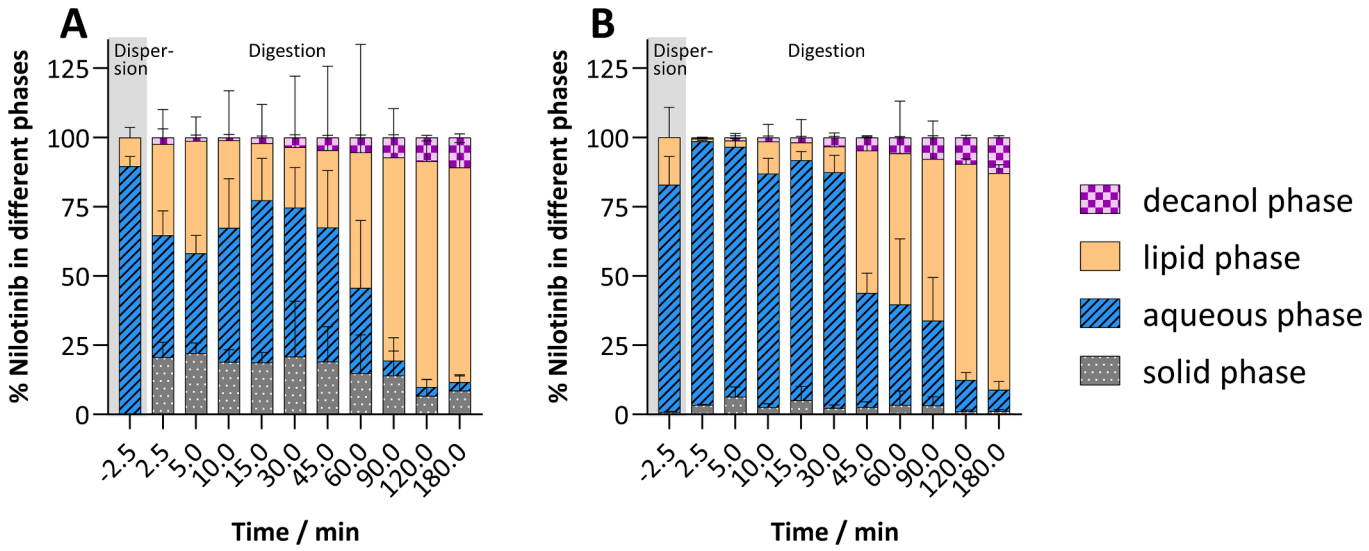


Fig. 4. Distribution of nilotinib during digestion of type III LBF with A: porcine pancreatin in calcium-free media B: with porcine pancreatin in calcium–containing media. Distribution is shown across the solid (grey, white dotted), aqueous (blue, striped), lipid (light orange) and decanol (purple, checkered) phase. They are based on the recovered amounts in these phases, except the lipid phase, which was calculated by subtracting the sum of recoveries in the other three phases from the total theoretical amount of nilotinib. The experiments were run with n = 3 and results are shown as mean + SD.

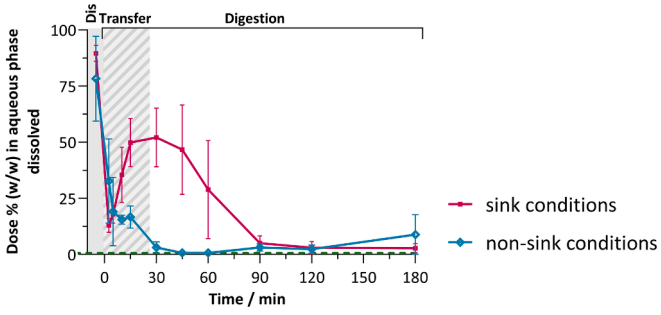


Fig. 5. Percentage of nilotinib in the aqueous phase dissolved, after addition of type III LBF in GI transfer lipolysis model with porcine pancreatin in calcium-free media under non-sink conditions (◊) and in the biphasic GI transfer lipolysis model under sink conditions (■). Means ± SD, n = 3.

examined to determine whether an absorptive sink can influence nilotinib concentration in the aqueous digest phase. An initial experiment determined that nilotinib solubility in decanol was 405 μg/mL after 24 h (see Fig. S2, Supplementary Materials). Subsequently, nilotinib was evaluated in a type III formulation (Section 2.2.4) in the GI transfer lipolysis model under sink conditions (with a decanol layer) and under non-sink conditions, using porcine pancreatin as the lipase source (see Figs. 5 and 6).

Under non–sink conditions, aqueous–phase concentrations of nilotinib declined rapidly upon transfer from the acidic gastric environment to intestinal digestion conditions. Overall concentrations of nilotinib in the aqueous digest phase corresponded to approximately 15–30% of the dose during the first 15 min and then drop to below 5%, remaining low for the remainder of the experiment (see Fig. 5). In contrast, under sink

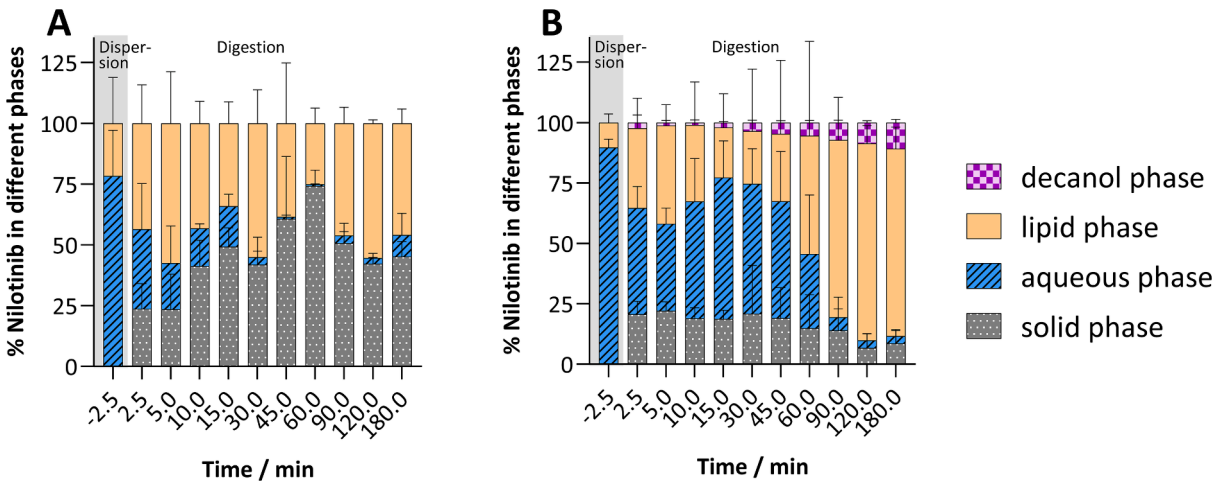


Fig. 6. Distribution of nilotinib during digestion of type III LBF in A: under non-sink conditions (GI transfer lipolysis model) and B: under sink conditions (biphasic GI transfer lipolysis model). Distribution is shown across the solid (grey, white dotted), aqueous (blue, striped), lipid (light orange) and decanol (purple, checkered) phase. They are based on the recovered amounts in these phases, except the lipid phase, which was calculated by subtracting the sum of recoveries in the other phases from the total theoretical amount of nilotinib. The experiments were run with n = 3 and results are shown as mean + SD.

conditions the apparent concentration of nilotinib in the aqueous digest phase was considerably higher, with 52.2 ± 13.1% of dose in the aqueous digest media determined after 30 min, followed by a relatively slower decline to ~ 5% of the dose after 90 min of digestion. Following ultracentrifugation of the digestion samples and quantification of nilotinib distribution across the solid, lipid, and aqueous phases (see Fig. 6), substantially greater drug precipitation was observed under non–sink conditions compared with sink conditions. This finding was consistent with the reduced precipitation detected when an absorptive sink is incorporated. The incorporation of the decanol phase sustains higher aqueous concentration over time and lowers the thermodynamic driving force for precipitation. These findings are in line with the study by Jede et al. (2023), where the addition of an absorptive compartment was able to enhance the accuracy of drug supersaturation predictions and it reduced overestimation of precipitation compared to classical USP II transfer model.

3.1.4. *Influence of lipase type in lipid free conditions*

Because porcine pancreatin contains multiple enzymatic and non–enzymatic constituents that may confound interpretation, the effect of enzyme source on nilotinib partitioning was investigated in the absence of an LBF. In addition to the commonly used porcine pancreatin, two other lipase sources were evaluated in the biphasic GI transfer lipolysis model. Palatase® 20000 L was chosen because it showed similar digestion kinetics to porcine pancreatin, and it led to similar aqueous fenofibrate concentrations during *in vitro* lipolysis of a LBF (Ejskjaer et al., 2024). Novozym® 435 was chosen to test whether an immobilized lipase was suitable for a biphasic system. Experiments were performed using nilotinib pre-dissolved in SGF in the absence of LBFs and under calcium-free conditions, with a no-enzyme control included.

As shown in Fig. 7A, nilotinib partitioning into decanol followed a similar slow, steady profile with both porcine pancreatin and Palatase® 20000 L, reaching approximately 22–27% of the dose in the decanol layer. Although porcine pancreatin contains a complex mixture of enzymes and auxiliary proteins, Ejskjaer et al. (2024) reported similar digestion profiles for porcine pancreatin and Palatase® 20000 L when acting on medium- and long-chain lipids. This suggests that digestion of the lipids present in FaSSIF may progress similarly with both enzymes, resulting in a comparable microenvironment for nilotinib and thus similar partitioning behaviour.

In the case of Novozym® 435 and lipase free control experiments, nilotinib partitioned into the decanol phase significantly faster during the initial 60 min. Under both conditions, over 50% of the dose in the decanol layer was reached after 90 min (Fig. 7A). This showed that the partitioning rate of nilotinib into the decanol layer did not limit overall transfer. Consistent with these observations, the aqueous phase total fraction of nilotinib declined rapidly when Novozym® 435 was used (similar for lipase free control) whereas a more gradual decline was

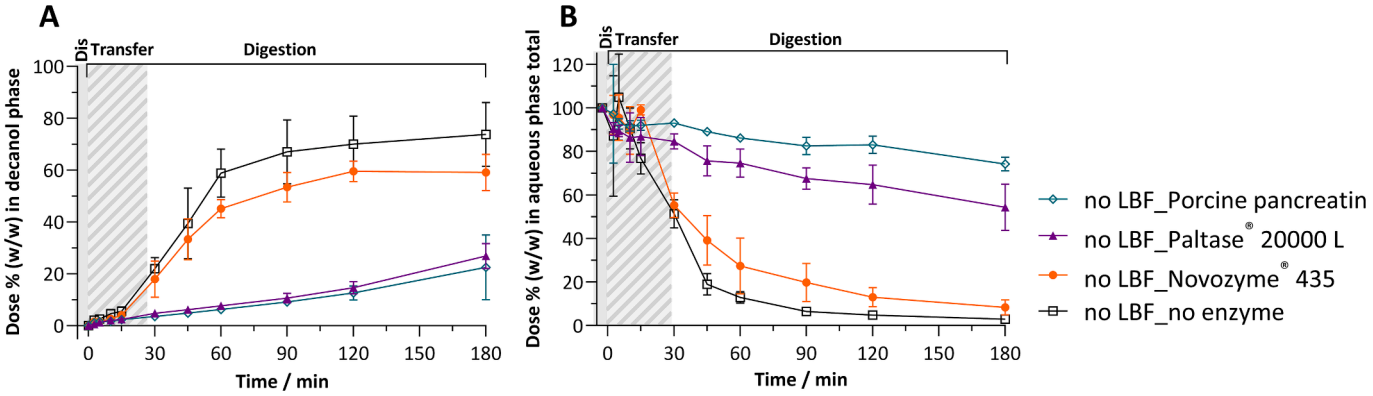


Fig. 7. Release profile of nilotinib in solution in SGF (no LBF present), in biphasic GI transfer lipolysis model. A: % of dose nilotinib in decanol phase and B: % of dose of nilotinib in aqueous phase total. Displayed are the tested enzymes: Palatase® 20000 L (▲), porcine pancreatin (◊), Novozym® 435 (●) and as control no lipase (□). Means ± SD, n = 3.

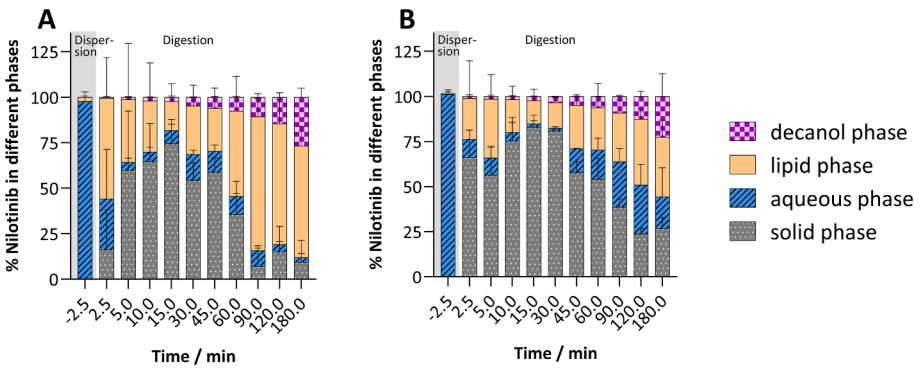


Fig. 8. Distribution of nilotinib during digestion of nilotinib solution (no LBF) with A: Palatase® 20000 L and B: Porcine pancreatin. Distribution is shown across the solid (grey, white dotted), aqueous (blue, striped), lipid (light orange) and decanol (purple, checkered) phase. They are based on the recovered amounts in these phases, except the lipid phase, which was calculated by subtracting the sum of recoveries in the other three phases from the total theoretical amount of nilotinib. The experiments were run with n = 3 and results are shown as mean + SD.

observed with porcine pancreatin and Palatase® 20000 L (Fig. 7B). When Novozym® 435 was employed, the immobilized enzyme beads tended to accumulate around the stirring paddle, migrate toward the aqueous–decanol interface, and intermittently enter the decanol phase (Fig. S5, Supplementary Materials). This aggregation and cross–phase contamination rendered Novozym® 435 unsuitable for use in a biphasic system.

With Palatase® 20000 L the maximum amount of nilotinib dissolved in the aqueous phase was reached earlier i.e. 13% at 30 min, immediately after GI transfer was completed (Fig. 8A). In contrast, when porcine pancreatin was present, the highest amount of nilotinib in the aqueous phase dissolved was observed, peaking above 25% between 90 and 120 min (Fig. 8B). Given the complex composition of the porcine pancreatin extract, it may be possible that its different components, such as residual lipids, contributed to an increased solubility of nilotinib in the aqueous phase (Grundy et al., 2021). It was observed that Palatase® 20000 L showed less variability in the aqueous phase percentage of drug. A possible explanation for this is the greater activity consistency and simpler handling compared with porcine pancreatin. Another advantage of using a liquid lipase was the potential to perform in-line UV detection in the aqueous phase (Ejskjaer et al., 2024). The average percentage of precipitated drug reached the maximum during the first half of the transfer for all conditions and subsequently decreased, with porcine pancreatin as lipase source nilotinib exhibited the highest and most sustained solid phase percentage throughout the experiment (see Fig. 8). The NaOH titration profiles were observed to be very similar (see Fig. S8, Supplementary Materials). The data revealed that both Palatase® 20000 L and porcine pancreatin were suitable lipase sources in this biphasic GI transfer lipolysis assay: porcine pancreatin promoted a more distinct supersaturation in the aqueous phase, whereas Palatase® 20000 L yielded lower variability in both the aqueous and decanol phases.

3.2. *Assessing influence of digestion of dispersible LBF on drug concentration in aqueous and absorptive sink*

To assess how digestion of a readily dispersible LBF influences drug levels in the aqueous and absorptive compartments, the effect of lipase source on nilotinib partitioning was evaluated using a LFCS type III formulation. Palatase® 20000 L was selected for the experiments based on observations in Section 3.1.4. In addition, supplementary experiments demonstrated that Palatase® 20000 L was also unaffected by presence or absence of calcium (Figs. S3 and S4). In the biphasic GI transfer lipolysis model, nilotinib exhibited a slow and steady partitioning behaviour into the organic layer (Fig. 9A). Up to the first 45 min similar concentrations in the decanol phase were measured with all four conditions. After 180 min 11% of the administered dose was present for porcine pancreatin and 19% for Palatase® 20000 L, being significantly different ($p < 0.05$). Under all conditions the highest proportion of drug in the aqueous digest phase were observed during the first 30 min of digestion (Fig. 9B). Upon completion of transfer, the percentage of dose that was dissolved in the aqueous phase decreased, as expected for a type III formulation, because digestion further lowers the solubilization capacity (Paulus et al., 2025). However, between 30 and 120 min, with porcine pancreatin a higher proportion of the drug was present in the aqueous phase relative to Palatase® 20000 L (Fig. 9B). Interestingly,

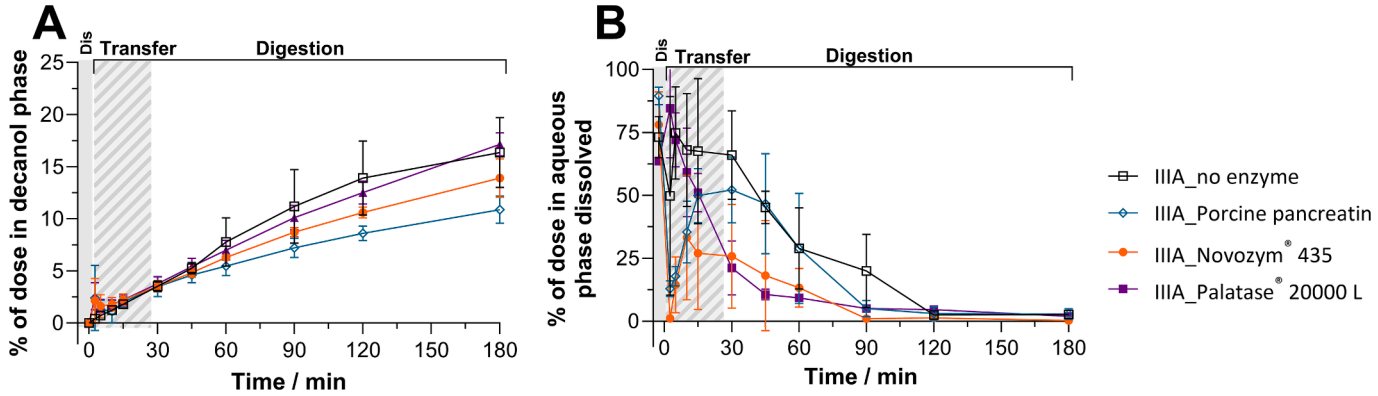


Fig. 9. Release profile of nilotinib in type III LBF, in biphasic GI transfer lipolysis model with A: % of dose nilotinib in decanol phase and B: % of dose of nilotinib in aqueous phase dissolved. Displayed are the tested lipase sources: Palatase® 20000 L (▲), porcine pancreatin (◊), Novozym® 435 (●) and as control no lipase (□). Means ± SD, n = 3.

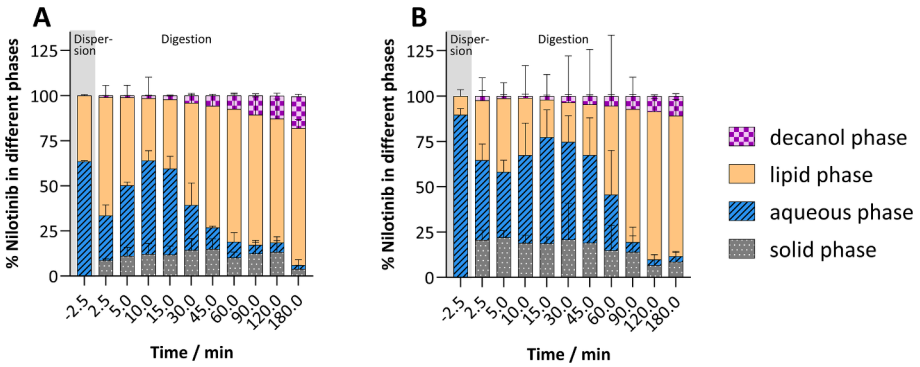


Fig. 10. Distribution of nilotinib during digestion of nilotinib in type III LBF in biphasic GI transfer lipolysis model with A: Palatase® 20000 L and B: Porcine pancreatin. Distribution is shown across the solid (grey, white dotted), aqueous (blue, striped), lipid (light orange) and decanol (purple, checkered) phase. They are based on the recovered amounts in these phases, except the lipid phase, which was calculated by subtracting the sum of recoveries in the other three phases from the total theoretical amount of nilotinib. The experiments were run with n = 3 and results are shown as mean + SD.

Table 3
Amount of FFAs (mmol) released during 180 min of digestion during biphasic GI transfer lipolysis experiment.[a]

Lipase source	Titrated FFAs released after 180 min of digestion [mmol]
Porcine pancreatin	0.341 ± 0.260
Palatase® 20000 L	0.675 ± 0.121
Novozym® 435	0.222 ± 0.047

[a] The amounts of released FFAs represent the values corrected for the level of FAs released during background lipolysis (digestion media alone). Means ± SD, n = 3.

when no lipases were added, the same trend of decrease after the 30 min mark in the aqueous phase dissolved was observed (Fig. 9B). As depicted in Fig. 10, the fraction of drug recovered as solid precipitate consistently remained below 25% across all tested conditions (drug distribution of no enzyme and Novozym® 435 in Fig. S7). This suggests that the reduction of drug percentage in the aqueous phase cannot be solely attributed to the precipitation. Furthermore, the percentage of drug absorbed into the decanol phase did not account for the entire decrease. Consequently, it is reasonable to infer that a significant portion of the drug resided within a micellar or lipid phase, which was separated from the aqueous phase during ultracentrifugation. Interestingly, there is an increase of drug in the lipid phase, also seen in Fig. 8, supporting the hypothesis that a level of decanol contamination into the aqueous phase occurred during the experiment. When the liquid lipase Palatase® 20000 L was used, the highest rate of digestion was measured (Table 3).

The findings indicated that the type III LBF reduced the driving force for nilotinib into the organic layer. The two non-ionic surfactants (Cremophor® RH40 and Tween® 85) acted as solubilizing agents and promoted micellization in the aqueous phase. This hypothesis is consistent with a previous biphasic diffusion study showing that increased micelle formation shifted drug distribution toward the aqueous phase (Dong et al., 2019). Collectively, these observations highlight that formulation composition controls partitioning kinetics in biphasic lipolysis assays. Experiments such as this incorporating both the decanol, aqueous and distribution of drug within the digest provide additional mechanistic insights on the dynamic interplay of how digestion changes over time. In future work, quantitative colloidal characterization (e.g., dynamic light scattering) could be performed to extend mechanistic understanding by revealing changes in hydrodynamic diameter and droplet polydispersity index (Jacobsen et al., 2023).

3.3. *Assessing influence of digestion of poorly dispersible LBF on drug concentration in aqueous phase and absorptive sink*

Subsequently to the well dispersible LBF we further investigated two poorly dispersible LBFs. These type I formulations were unsuitable to be tested in the biphasic GI transfer lipolysis set-up, since the LBFs were floating on top of the SGF and, consequently, could not reliably be transported through the tubing of the peristaltic pump (pictures are included in Fig. S1 in Supplementary Materials). Attempts to transfer the type I suspension resulted in substantial retention of lipid on the vessel wall. Therefore, a biphasic pH-shift lipolysis method was developed, based on O'Dwyer et al. (2020), described in Section 2.2.6. Two poorly dispersible Peceol®–based nilotinib formulations were evaluated: a type

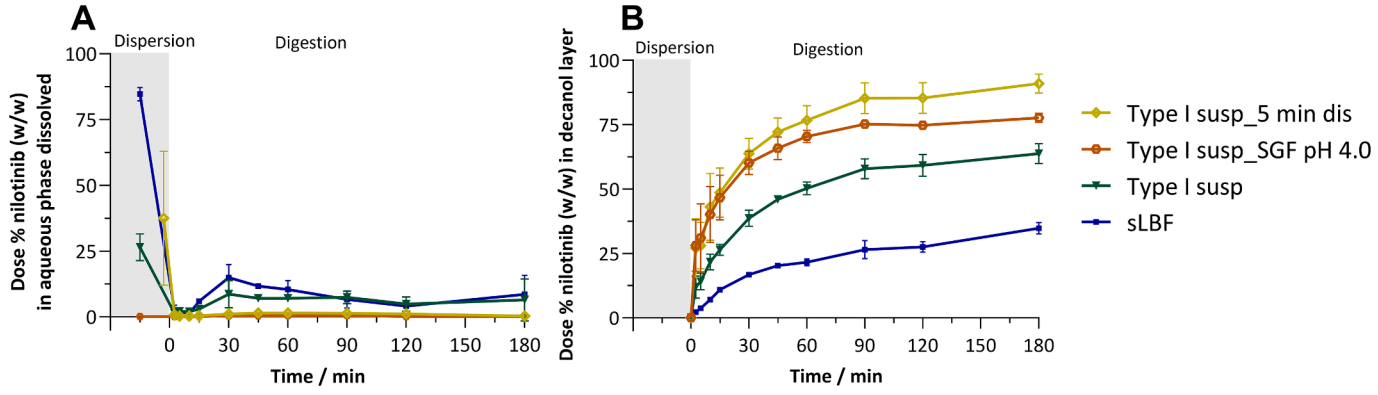


Fig. 11. Release profile of nilotinib in type I LBF, in biphasic pH-shift lipolysis model. Displayed are A: Nilotinib in % of dose in decanol phase and B: Nilotinib in % of dose in aqueous phase dissolved. sLBF tested with 30 min dispersion at pH 2.0 (■); type I suspension tested with: dispersion of 5 min in SGF at pH 2.0 (◊), 30 min in SGF at pH 2.0 (▼) and 30 min in SGF pH 4.0 (○). Means ± SD, n = 3.

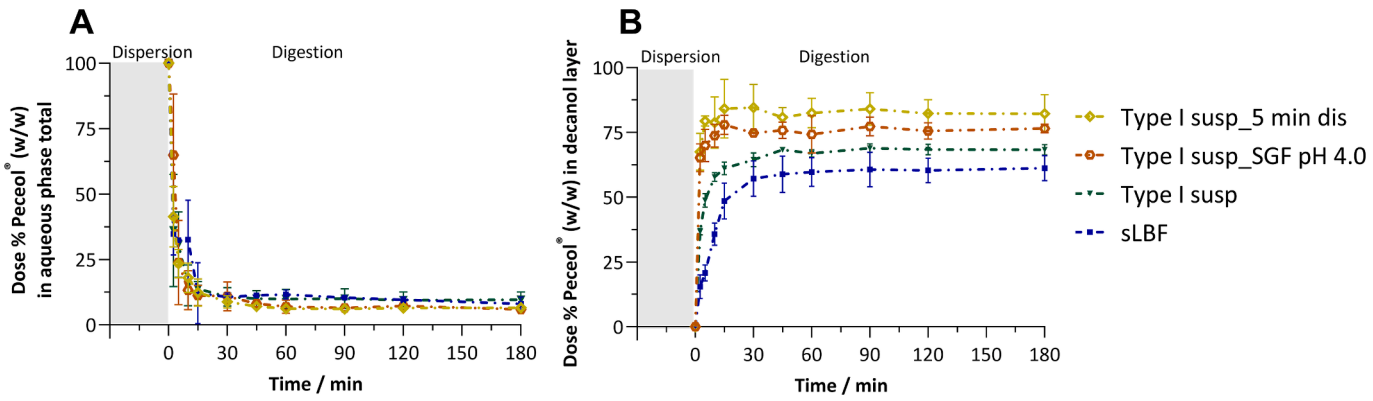


Fig. 12. Release profile of Peceol® of the type I formulations tested in biphasic pH-shift lipolysis setup. Displayed are A: Peceol® in % of dose in decanol phase and B: Peceol® in % of dose in aqueous phase total. sLBF tested with 30 min dispersion at pH 2.0 (■); type I suspension tested with: dispersion of 5 min in SGF at pH 2.0 (◊), 30 min in SGF at pH 2.0 (▼) and 30 min in SGF pH 4.0 (○). Means ± SD, n = 3.

I LBF suspension and a type I supersaturated LBF. The partitioning of drugs and lipid components into the organic compartment was analysed and evaluated (see Fig. 11A and B). When nilotinib was incorporated in the sLBF, 34.7 ± 2.2% of the dose partitioned into the decanol phase, whereas the type I suspension yielded a significantly greater partitioning with 63.7 ± 3.9% of dose ($p < 0.05$; Fig. 11B). The distribution of Peceol® between the aqueous and organic phases was broadly similar regardless of the formulation, i.e., suspension versus sLBF (Fig. 12A and B). In each case, more than 50% of Peceol® had partitioned into decanol within the first 15 min. These results support the hypothesis that undissolved nilotinib particles are coated with Peceol, enabling their direct transfer into decanol. This observation correlated with observations by O'Dwyer et al. (2020) for nilotinib dispersed in olive oil, i.e., direct mixing of the type I oil into the decanol layer due to incomplete dispersion.

Additionally, the LBF type I suspension was studied with two dispersion times (5 min versus 30 min) and two SGF pH values (pH 2.0 versus 4.0) during dispersion, to elucidate how dispersion conditions affected subsequent supersaturation, precipitation and partitioning. Reducing the dispersion time from 30 min to 5 min markedly accelerated the transfer of both Peceol® and nilotinib into the organic phase, leading to the highest percentage of dose for both analytes (Figs. 11 and 12AsA). With a dispersion at pH 4.0, where nilotinib showed a significantly lower aqueous solubility (see Fig. 11A), accelerated transfer of Peceol® and nilotinib into the decanol layer was observed. The observed rank order of percentage of dose for both nilotinib and Peceol® in decanol is type I susp_5 min dispersion > type I susp_SGF pH 4.0 > type I susp > sLBF.

In all experiments more than 50% of the added Peceol® was recovered in the organic phase, indicating a good mixability of Peceol® and decanol (see Fig. 12B). This observation was supported by calculated Hansen solubility parameters: for glyceryl oleate (predominant fraction of Peceol®) = 19.36 $MPa^{1/2}$ and for decanol = 20.43 $MPa^{1/2}$. The calculated Hansen solubility parameters of glyceryl oleate and decanol were very similar, indicating the favourable miscibility of the two substances (Hansen, 2007). These calculations were performed retrospectively to support the experimental finding that Peceol® had rapidly partitioned into decanol. For future studies, prospective calculation of Hansen's three–dimensional solubility parameters could be used to predict whether a given lipid excipient is likely to partition into decanol. The one–compartment approach is fit–for–purpose for poorly dispersible systems, further refinement (e.g., lipid quantification in the decanol layer, interface control, or alternative sink phases) may be required to mitigate lipid/drug co–transfer and strengthen interpretability.

For Type I LBFs, drug transfer into the decanol layer reflects both molecularly dissolved drug and potentially drug co–partitioning with formulation lipids that partition into the organic phase. This interpretation aligns with findings of Dening et al. (2019); who reported partitioning of lipolytic products and an encapsulated drug between the aqueous phase and pellet during lipolysis. Consequently, extensive lipid partitioning in poorly dispersible formulations indicates lipid carryover rather than true physiological absorption; therefore, interpretations of the overall flux are limited.

The findings underscore the need for this study to enhance the understanding of biphasic lipolysis assays for assessing the performance of LBFs, thereby facilitating more informed formulation development strategies. Suitable conditions were established for evaluating the lipolysis of LBFs during a dynamic pH transition in the presence of an absorptive sink. To further strengthen these findings, the same experimental framework should be expanded to include additional APIs and a broader range of LBF types. For formulations containing long-chain lipids, where direct transfer of drug into the organic phase can occur, quantification of lipid components using ELSD is recommended to determine whether drug partitioning is driven by lipid carryover. Using ELSD also allowed detection of decanol in the aqueous phase, confirming partial dispersion of the organic layer during the experiment. Prospective use of physicochemical predictors, such as Hansen solubility parameters, may also help identify lipid excipients that are more likely to mix with the organic phase. Moreover, integrating biphasic lipolysis data with PBPK modelling could offer a practical means to assess and refine the predictive performance of the assay and to define fit-for-purpose experimental conditions (O'Dwyer et al., 2019). Ultimately, comparing *in vitro* outcomes for multiple LBF types across drugs that capture a wide range of physiochemical properties, with corresponding *in vivo* performance data, will be essential for establishing the predictive value of these biphasic lipolysis methods in formulation development.

4. Conclusions

In this study, a biphasic GI transfer and a biphasic pH-shift lipolysis model that combined a physiological GI transfer or a rapid pH-shift with an organic absorptive compartment were established to explore lipolysis of a LBF under dynamic GI transfer and digestion conditions. The incorporation of a decanol overlay provided effective sink conditions and reduced drug precipitation in the aqueous digest phase. Importantly this study demonstrated that the decanol layer did not reduce lipase activity and liberation of free fatty acids during digestion did not impede nilotinib partitioning into the decanol layer. The study established conditions for using both Palatase® 20000 L and porcine pancreatin to mimic digestion in the biphasic GI transfer model, whereas Novozym® 435 was unsuitable. For a readily dispersible LFCS type III formulation drug partitioning into decanol was gradual and differences were observed in how the choice of lipase appears to influence the rate at

which the drug can partition into the decanol layer, with Palatase® 20000 L higher percentages of drug were found. For poorly dispersible Type I systems, the one–compartment biphasic pH–shift setup was the more appropriate choice, but it also carries an ongoing risk of lipid carryover and entrapped crystalline drug transferring into the organic phase, which may bias partitioning readouts. The study highlights the importance of tracking the drug distribution within the various digest phases to monitor how drug is transitioning out of the aqueous phase into the lipid and or decanol phase. Overall, this work provided practical guidance on experimental parameter selection and highlighted mechanistic factors that must be considered when applying biphasic *in vitro* lipolysis models to evaluate LBFs. The study further underscored the need to select or design lipolysis models that are fit for purpose for the specific LBF class.

CRediT authorship contribution statement

Hannah S. Kirschbaum: Writing – review & editing, Writing – original draft, Visualization, Validation, Project administration, Methodology, Investigation, Formal analysis, Conceptualization. **Christian Jede:** Writing – review & editing, Validation, Supervision, Resources, Project administration, Methodology, Conceptualization. **Laura J. Koehl:** Writing – review & editing, Validation, Supervision, Methodology, Conceptualization. **Martin Kuentz:** Writing – review & editing, Validation, Supervision, Methodology, Conceptualization. **René Holm:** Writing – review & editing, Validation, Supervision, Methodology, Conceptualization. **Brendan T. Griffin:** Writing – review & editing, Validation, Supervision, Methodology, Conceptualization. **Johannes A. Blechar:** Writing – review & editing, Validation, Supervision, Project administration, Methodology, Conceptualization. **Patrick J. ÓDwyer:** Writing – review & editing, Validation, Supervision, Project administration, Methodology, Conceptualization.

Funding

This research did not receive any specific grant from funding agencies in the public, commercial, or not-for-profit sectors.

Declaration of Generative AI and AI-assisted technologies.

During the preparation of this work the author used (MyGPT-suite/Merck KGaA) to improve readability and language. After using this tool, the author reviewed and edited the content as needed and takes full responsibility for the content of the publication.

Declaration of competing interest

The authors declare that they have no known competing financial interests or personal relationships that could have appeared to influence the work reported in this paper.

Acknowledgement

The authors thank Tobias Nolte for the support with 3D-printing of paddles and lids for the dissolution vessel. Furthermore, they like to thank Tobias Lieblein for his help with the ELSD method development.

Appendix A. Supplementary data

Supplementary data to this article can be found online at https://doi.org/10.1016/j.ijpharm.2026.127051.

Data availability

Data will be made available on request.

References

Ting, J.M., Porter 3rd, W.W., Mecca, J.M., Bates, F.S., Reineke, T.M., 2018. Advances in polymer design for enhancing oral drug solubility and delivery. Bioconjug. Chem. 29 (4), 939–952. https://doi.org/10.1021/acs.bioconjchem.7b00646.

Hashmi, A.R., Sekar, M., Zahra, F., Molugulu, N., Wong, L.S., 2025. Advanced drug delivery strategies to overcome solubility and permeability challenges: driving biopharmaceutical advancements toward commercial success. ACS Omega 10 (36), 40769–40792. https://doi.org/10.1021/acsomega.5c06171.

Stegemann, S., Moreton, C., Svanback, S., Box, K., Motte, G., Paudel, A., 2023. Trends in oral small-molecule drug discovery and product development based on product launches before and after the rule of five. Drug Discov. Today 28 (2), 103344. https://doi.org/10.1016/j.drudis.2022.103344.

Kuentz, M., Holm, R., Kronseder, C., Saal, C., Griffin, B.T., 2021. Rational selection of bio-enabling oral drug formulations - a PEARRL commentary. J. Pharm. Sci. 110 (5), 1921–1930. https://doi.org/10.1016/j.xphs.2021.02.004.

Feeney, O.M., Crum, M.F., McEvoy, C.L., Trevaskis, N.L., Williams, H.D., Pouton, C.W., Charman, W.N., Bergstrom, C.A.S., Porter, C.J.H., 2016. 50years of oral lipid-based formulations: provenance, progress and future perspectives. Adv. Drug Deliv. Rev. 101, 167–194. https://doi.org/10.1016/j.addr.2016.04.007.

Bourderi-Cambon, A., Fadhlaoui, K., Garrait, G., Laine, E., Dhifallah, I., Rossano, M., Caisse, P., Beyssac, E., 2025. Improving in vitro-in vivo correlation (IVIVC) for lipid-based formulations. Overcoming Challenges and Exploring Opportunities. Pharmaceutics 17 (10). https://doi.org/10.3390/pharmaceutics17101310.

Bennett-Lenane, H., O'Shea, J.P., O'Driscoll, C.M., Griffin, B.T., 2020. A retrospective biopharmaceutical analysis of >800 approved oral drug products: are drug properties of solid dispersions and lipid-based formulations distinctive? J. Pharm. Sci. 109 (11), 3248–3261. https://doi.org/10.1016/j.xphs.2020.08.008.

Ueda, K., Porter, C.J.H., Goodwin, A., Taylor, L.S., 2026. The expanding role of formulations to enable oral delivery of poorly water-soluble drugs. Nat. Rev. Drug Discov. https://doi.org/10.1038/s41573-026-01407-5.

Berthelsen, R., Klitgaard, M., Rades, T., Mullertz, A., 2019. In vitro digestion models to evaluate lipid based drug delivery systems; present status and current trends. Adv. Drug Deliv. Rev. 142, 35–49. https://doi.org/10.1016/j.addr.2019.06.010.

Weinheimer, M., Fricker, G., Burhenne, J., Mylius, P., Schubert, R., 2017. The application of P-gp inhibiting phospholipids as novel oral bioavailability enhancers - an in vitro and in vivo comparison. Eur. J. Pharm. Sci. 108, 13–22. https://doi.org/10.1016/j.ejps.2016.08.055.

Lindmark, T., Kimura, Y., Artursson, P., 1998. Absorption enhancement through intracellular regulation of tight junction permeability by medium chain fatty acids in Caco-2 cells. J. Pharmacol. Exp. Ther. 284 (1), 362–369. https://doi.org/10.1016/s0022-3565(24)37216-7.

Vinarov, Z., Abrahamsson, B., Artursson, P., Batchelor, H., Berben, P., Bernkop-Schnurch, A., Butler, J., Ceulemans, J., Davies, N., Dupont, D., et al., 2021. Current challenges and future perspectives in oral absorption research: an opinion of the UNGAP network. Adv. Drug Deliv. Rev. 171, 289–331. https://doi.org/10.1016/j.addr.2021.02.001.

O'Dwyer, P.J., Litou, C., Box, K.J., Dressman, J.B., Kostewicz, E.S., Kuentz, M., Reppas, C., 2019. In vitro methods to assess drug precipitation in the fasted small intestine - a PEARRL review. J. Pharm. Pharmacol. 71 (4), 536–556. https://doi.org/10.1111/jphp.12951.

Sek, L., Porter, C.J., Kaukonen, A.M., Charman, W.N., 2002. Evaluation of the in-vitro digestion profiles of long and medium chain glycerides and the phase behaviour of their lipolytic products. J. Pharm. Pharmacol. 54 (1), 29–41. https://doi.org/10.1211/0022357021771896.

Zangenberg, N.H., Müllertz, A., Kristensen, H.G., Hovgaard, L., 2001. A dynamic in vitro lipolysis model I. Controlling the rate of lipolysis by continuous addition of calcium. Eur. J. Pharm. Sci. 14, 115–122. https://doi.org/10.1016/S0928-0987(01)00169-5.

Williams, H.D., Sassene, P., Kleberg, K., Bakala-N'Goma, J.C., Calderone, M., Jannin, V., Igonin, A., Partheil, A., Marchaud, D., Jule, E., et al., 2012. Toward the establishment of standardized in vitro tests for lipid-based formulations, part 1: method parameterization and comparison of in vitro digestion profiles across a range of representative formulations. J. Pharm. Sci. 101 (9), 3360–3380. https://doi.org/10.1002/jps.23205.

Griffin, B.T., Kuentz, M., Vertzoni, M., Kostewicz, E.S., Fei, Y., Faisal, W., Stillhart, C., O'Driscoll, C.M., Reppas, C., Dressman, J.B., 2014. Comparison of in vitro tests at various levels of complexity for the prediction of in vivo performance of lipid-based formulations: case studies with fenofibrate. Eur. J. Pharm. Biopharm. 86 (3), 427–437. https://doi.org/10.1016/j.ejpb.2013.10.016.

Kirschbaum, H.S., Koehl, N.J., Blechar, J.A., Wiesinger, C., Koehl, L.J., PJ, O.D., Kuentz, M., Holm, R., Jede, C., Griffin, B.T., 2025. pH-stat versus pH-shift lipolysis model: exploring in vitro-in vivo relationships for lipid-based formulations of nilotinib. Eur. J. Pharm. Sci. 214, 107250. https://doi.org/10.1016/j.ejps.2025.107250.

Fernandez, S., Chevrier, S., Ritter, N., Mahler, B., Demarne, F., Carriere, F., Jannin, V., 2009. In vitro gastrointestinal lipolysis of four formulations of piroxicam and cinnarizine with the self emulsifying excipients Labrasol and Gelucire 44/14. Pharm. Res. 26 (8), 1901–1910. https://doi.org/10.1007/s11095-009-9906-2.

Klitgaard, M., Beilles, S., Sassene, P.J., Berthelsen, R., Mullertz, A., 2020. Adding a gastric step to the intestinal in vitro digestion model improves the prediction of pharmacokinetic data in beagle dogs of two lipid-based drug delivery systems. Mol. Pharm. 17 (9), 3214–3222. https://doi.org/10.1021/acs.molpharmaceut.0c00307.

Siqueira Jorgensen, S.D., Al Sawaf, M., Graeser, K., Mu, H., Mullertz, A., Rades, T., 2018. The ability of two in vitro lipolysis models reflecting the human and rat gastrointestinal conditions to predict the in vivo performance of SNEDDS dosing regimens.

Eur. J. Pharm. Biopharm. 124, 116–124. https://doi.org/10.1016/j.ejpb.2017.12.014.
Christophersen, P.C., Christiansen, M.L., Holm, R., Kristensen, J., Jacobsen, J., Abrahamsson, B., Mullertz, A., 2014. Fed and fasted state gastro-intestinal in vitro lipolysis: in vitro in vivo relations of a conventional tablet, a SNEDDS and a solidified SNEDDS. Eur. J. Pharm. Sci. 57, 232–239. https://doi.org/10.1016/j.ejps.2013.09.007.
Fiolka, T., Abeele, J.V.D., Augustijns, P., Arora, S., Dressman, J., 2020. Biorelevant two-stage in vitro testing for rDCS classification and in PBPK modeling–case example ritonavir. Pharmaceutics, Drug Delivery and Pharmaceutical Technol. 109 (8), 2512–2526. https://doi.org/10.1016/j.xphs.2020.04.023.
Siqueira Jorgensen, S., Rades, T., Mu, H., Graeser, K., Mullertz, A., 2019. Exploring the utility of the chasing principle: influence of drug-free SNEDDS composition on solubilization of carvedilol, cinnarizine and R3040 in aqueous suspension. Acta Pharm. Sin. B 9 (1), 194–201. https://doi.org/10.1016/j.apsb.2018.07.004.
Sassene, P.J., Michaelsen, M.H., Mosgaard, M.D., Jensen, M.K., Van Den Broek, E., Wasan, K.M., Mu, H., Rades, T., Mullertz, A., 2016. In vivo precipitation of poorly soluble drugs from lipid-based drug delivery systems. Mol. Pharm. 13 (10), 3417–3426. https://doi.org/10.1021/acs.molpharmaceut.6b00413.
Stillhart, C., Kuentz, M., 2016. Trends in the assessment of drug supersaturation and precipitation in vitro using lipid-based delivery systems. J. Pharm. Sci. 105 (9), 2468–2476. https://doi.org/10.1016/j.xphs.2016.01.010.
Sironi, D., Rosenberg, J., Bauer-Brandl, A., Brandl, M., 2018. PermeaLoop, a novel in vitro tool for small-scale drug-dissolution/permeation studies. J. Pharm. Biomed. Anal. 156, 247–251. https://doi.org/10.1016/j.jpba.2018.04.042.
Sirvi, A., Jadhav, K., Sangamwar, A.T., 2024. Enabling superior drug loading in lipid-based formulations with lipophilic salts for a brick dust molecule: exploration of lipophilic counterions and in vitro-in vivo evaluation. Int. J. Pharm. 656, 124108. https://doi.org/10.1016/j.ijpharm.2024.124108.
Klitgaard, M., Mullertz, A., Berthelsen, R., 2021. Estimating the oral absorption from self-nanoemulsifying drug delivery systems using an in vitro lipolysis-permeation method. Pharmaceutics 13 (4). https://doi.org/10.3390/pharmaceutics13040489.
Lopez Marmol, A., Barker, R., Koziolek, M., Schwabe, R., Hens, B., Sarcevica, I., Butler, J. M., McAllister, M., Taylor, E., Chiang, P.C., et al., 2026. An expert's view on the application of TIM technology in the development of oral drug products. Mol. Pharm. https://doi.org/10.1021/acs.molpharmaceut.5c01197.
Brenner, M.B., Wüst, M., Frank, J., Wagner, K.G., 2024. In vivo predictive dissolution of the lipophilic phytochemicals trans-resveratrol, coenzyme Q10 and quercetin. J. Drug Delivery Sci. Technol. 95. https://doi.org/10.1016/j.jddst.2024.105561.
Mudie, D.M., Shi, Y., Ping, H., Gao, P., Amidon, G.L., Amidon, G.E., 2012. Mechanistic analysis of solute transport in an in vitro physiological two-phase dissolution apparatus. Biopharm. Drug Dispos. 33 (7), 378–402. https://doi.org/10.1002/bdd.1803.
Deng, J., Staufenbiel, S., Bodmeier, R., 2017. Evaluation of a biphasic in vitro dissolution test for estimating the bioavailability of carbamazepine polymorphic forms. Eur. J. Pharm. Sci. 105, 64–70. https://doi.org/10.1016/j.ejps.2017.05.013.
Denninger, A., Westedt, U., Rosenberg, J., Wagner, K.G., 2020. A rational design of a biphasic dissolutionsetup-modelling of biorelevant kinetics for a ritonavir hot-melt extruded amorphous solid dispersion. Pharmaceutics 12 (3). https://doi.org/10.3390/pharmaceutics12030237.
Jede, C., Henze, L.J., Meiners, K., Bogdahn, M., Wedel, M., van Axel, V., 2023. Development and application of a dissolution-transfer-partitioning system (DTPS) for biopharmaceutical drug characterization. Pharmaceutics 15 (4). https://doi.org/10.3390/pharmaceutics15041069.
O'Dwyer, P.J., Box, K.J., Koehl, N.J., Bennett-Lenane, H., Reppas, C., Holm, R., Kuentz, M., Griffin, B.T., 2020. Novel biphasic lipolysis method to predict in vivo performance of lipid-based formulations. Mol. Pharm. 17 (9), 3342–3352. https://doi.org/10.1021/acs.molpharmaceut.0c00427.
Mathias, N.R., Xu, Y., Patel, D., Grass, M., Caldwell, B., Jager, C., Mullin, J., Hansen, L., Crison, J., Saari, A., et al., 2013. Assessing the risk of pH-dependent absorption for new molecular entities: a novel in vitro dissolution test, physicochemical analysis, and risk assessment strategy. Mol. Pharm. 10 (11), 4063–4073. https://doi.org/10.1021/mp400426f.
Koehl, N.J., Holm, R., Kuentz, M., Griffin, B.T., 2019. New insights into using lipid based suspensions for 'Brick Dust' molecules: case study of Nilotinib. Pharm. Res. 36 (4), 56. https://doi.org/10.1007/s11095-019-2590-y.
Jede, C., Wagner, C., Kubas, H., Weigandt, M., Weber, C., Lecomte, M., Badolo, L., Koziolek, M., Weitschies, W., 2019. Improved prediction of in vivo supersaturation and precipitation of poorly soluble weakly basic drugs using a biorelevant bicarbonate buffer in a gastrointestinal transfer model. Mol. Pharm. 16 (9), 3938–3947. https://doi.org/10.1021/acs.molpharmaceut.9b00534.
Grundy, M.M.L., Abrahamse, E., Almgren, A., Alminger, M., Andres, A., Ariëns, R.M.C., Bastiaan-Net, S., Bourlieu-Lacanal, C., Brodkorb, A., Bronze, M.R., et al., 2021. INFOGEST inter-laboratory recommendations for assaying gastric and pancreatic lipases activities prior to in vitro digestion studies. J. Funct. Foods 82. https://doi.org/10.1016/j.jff.2021.104497.
Bennett-Lenane, H., Jorgensen, J.R., Koehl, N.J., Henze, L.J., O'Shea, J.P., Mullertz, A., Griffin, B.T., 2021. Exploring porcine gastric and intestinal fluids using microscopic and solubility estimates: impact of placebo self-emulsifying drug delivery system administration to inform bio-predictive in vitro tools. Eur. J. Pharm. Sci. 161, 105778. https://doi.org/10.1016/j.ejps.2021.105778.
Ejskjaer, L., O'Dwyer, P.J., Ryan, C.D., Holm, R., Kuentz, M., Box, K.J., Griffin, B.T., 2024. Developing an in vitro lipolysis model for real-time analysis of drug concentrations during digestion of lipid-based formulations. Eur. J. Pharm. Sci. 194, 106681. https://doi.org/10.1016/j.ejps.2023.106681.
Keemink, J., Bergstrom, C.A.S., 2018. Caco-2 cell conditions enabling studies of drug absorption from digestible lipid-based formulations. Pharm. Res. 35 (4), 74. https://doi.org/10.1007/s11095-017-2327-8.
Mousli, Y., Brachet, M., Chain, J.L., Ferey, L., 2022. A rapid and quantitative reversed-phase HPLC-DAD/ELSD method for lipids involved in nanoparticle formulations. J. Pharm. Biomed. Anal. 220, 115011. https://doi.org/10.1016/j.jpba.2022.115011.
Reis, P., Holmberg, K., Watzke, H., Leser, M.E., Miller, R., 2009. Lipases at interfaces: a review. Adv. Colloid Interface Sci. 147–148, 237–250. https://doi.org/10.1016/j.cis.2008.06.001.
Devraj, R., Williams, H.D., Warren, D.B., Mullertz, A., Porter, C.J., Pouton, C.W., 2013. In vitro digestion testing of lipid-based delivery systems: calcium ions combine with fatty acids liberated from triglyceride rich lipid solutions to form soaps and reduce the solubilization capacity of colloidal digestion products. Int. J. Pharm. 441 (1–2), 323–333. https://doi.org/10.1016/j.ijpharm.2012.11.024.
Paulus, F., Bauer-Brandl, A., Stappaerts, J., Holm, R., 2025. Continuing along the lipid formulation classification system: effects of lipid chain length, supersaturation, digestion, and precipitation inhibition on cinnarizine absorption from type IIIa lipid-based formulations. Int. J. Pharm. 678, 125712. https://doi.org/10.1016/j.ijpharm.2025.125712.
Dong, Y., Hengst, L., Patel, D., Hunt, R., Qu, H., Choi, S., Ashraf, M., Cruz, C.N., Xu, X., 2019. A kinetic approach to determining drug distribution in complex biphasic systems. J. Pharm. Sci. 108 (6), 2002–2011. https://doi.org/10.1016/j.xphs.2019.01.003.
Jacobsen, A.C., Kabedev, A., Sinko, P.D., Palm, J.E., Bergstrom, C.A.S., Teleki, A., 2023. Intrinsic lipolysis rate for systematic design of lipid-based formulations. Drug Deliv. Transl. Res. 13 (5), 1288–1304. https://doi.org/10.1007/s13346-022-01246-y.
Hansen, C. M. Hansen Solubility Parameters: A User's Handbook, Second Edition; CRC Press., 2007. DOI: https://doi.org/10.1201/9781420006834.
Dening, T.J., Joyce, P., Prestidge, C.A., 2019. Improving correlations between drug solubilization and in vitro lipolysis by monitoring the phase partitioning of lipolytic species for lipid-based formulations. J. Pharm. Sci. 108 (1), 295–304. https://doi.org/10.1016/j.xphs.2018.09.016.